

Elastic matching based on motion vector fields obtained with a histogram-based similarity measure for DSA-image correction

Thorsten M. Buzug, Jürgen Weese, Carola Fassnacht and Cristian Lorenz

Philips Research Hamburg,
Röntgenstraße 24-26, 22335 Hamburg, Germany
buzug@pfh.research.philips.com

1. INTRODUCTION

It is well known that enhancement of digital subtraction angiography (DSA) images is essentially a registration task [1], i.e. mask and contrast image must be matched before subtraction to reduce artifacts that arise from patient movement. Most of the current algorithms are point-based registration methods using motion vector fields obtained by template- or block-matching procedures [2,3,4]. However, the main problem of such registration strategies is, that mask and contrast image are dissimilar to a certain extent due to the injection of contrast agent during image acquisition.

Recently, similarity measures have been introduced obtained from weighted one-dimensional histograms that are especially suitable for these dissimilarities in DSA [5]. It has been mathematically proven that any convex weighting function is appropriate to measure the degree of misregistration [6]. Furthermore, it has been shown that this class of similarity measures is better adapted to the gray-value distortions in DSA images than other well-known similarity measures such as cross correlation [7], sum of absolute differences [8], and deterministic sign change [2,3]. In particular, the histogram-based similarity measures lead to a very smooth motion vector field, i.e. the number of outliers in the motion vector field is significantly reduced compared with the usually employed measures. With respect to computational efficiency we used the (strictly) convex energy function for the similarity measure presented in this paper. The motion vector field supplies us with a set of homologous landmarks that is used for point-based registration. Results are presented for image pairs corrected with an affine transformation, where the patient-induced distortions could be reduced. However, patient motion is often more complex. Especially for abdominal images, it has been shown that residual artifacts are visible in the subtraction images even after an affine correction. Therefore, higher-order polynomial or even more flexible transformations must be applied. In this paper, we present the results of an elastic registration based on thin-plate splines [9]. This interpolation approach can be used thanks to the very smooth motion vector fields that are estimated with sub-pixel accuracy.

2. DSA ALGORITHM

While in clinical routine an interactive shifting procedure is established to compensate for patient movement artifacts, here, a correction has been proposed based on motion vector fields. The main problem for the estimation of the motion vector field is the choice of an appropriate similarity measure [4,5], because mask and contrast image are dissimilar due to injection of contrast agent. Recently, similarity measures have been introduced, obtained from

weighted one-dimensional histograms that are optimally adapted to the dissimilarities of DSA [6]. Such measures are defined in a 3-step procedure that consists in: (i) subtraction of images inside a quadratic block that is called template, (ii) calculation of gray-value histogram of the difference image and normalization of the histogram according to $\sum p_k=1$, where p_k is the fraction of pixels with gray-value g_k , (the fraction of pixels depends on the shift parameters r and s , i.e. $p_k=p_k(r,s)$), and (iii) evaluation of similarity measure $M(r,s)=\sum h(p_k)$, using an appropriately defined weighting function $h(p)$. It has been shown that the energy similarity measure, the sum of the squared histogram values, i.e. $h(p_k)=p_k^2$, turned out to be the most suitable measure for template matching and is consequently used in this paper.

Sub-pixel correction is often required for shift procedures, because if there is misregistration, even of less than one pixel width, the subtraction operation is similar to a differentiation [10]. This may lead to strong distortions at the edges of objects in the subtraction image. This is especially important, if interpolation procedures are applied for image correction. Two approaches to obtain the parameters of a sub-pixel shift are possible. On the one hand the templates in the mask and corresponding contrast image can be interpolated and then shifted on a sub-pixel grid. This method is very time consuming and, therefore, not used here. On the other hand a quadratic approximation of the similarity measure in the vicinity of the extremum (estimated in pixel accuracy) can be used to obtain sub-pixel shift estimates. This is a faster approach than interpolation of the image data. An 8-neighbourhood is used of the similarity measure optimum, i.e. the maximum of the energy similarity measure, to fit a quadratic function. The parameters of the function

$$M(x,y)=b_0 + b_1x + b_2y + b_3x^2 + b_4xy + b_5y^2 \quad (1)$$

are computed using singular value decomposition [11]. Hence, the optimum of that approximated quadratic function yields the estimates for the sub-pixel shift:

$$s_{\min} = \frac{2b_3b_2 - b_1b_4}{b_4^2 - 4b_3b_5} \quad \text{and} \quad r_{\min} = -\frac{s_{\min}b_4 + b_1}{2b_3} \quad (2a/b)$$

Fig. 1 illustrates the approximation of eq. (1) to the objective function (the energy similarity measure) obtained from a template that is shifted in an image pair of the abdomen. The grid represents the values of the pixel-accurate energy similarity measure. For visualization purposes the energy measure is inverted in this illustration. The gray-value coded surface of the approximated quadratic function (1) is overlaid to the grid of pixel-accurate energy values. It can be seen that the extremum of the approximated quadratic function (indicated as black circle) is slightly shifted with respect to the pixel extremum of the energy similarity measure which can be found at $(r,s)=(0,-9)$.

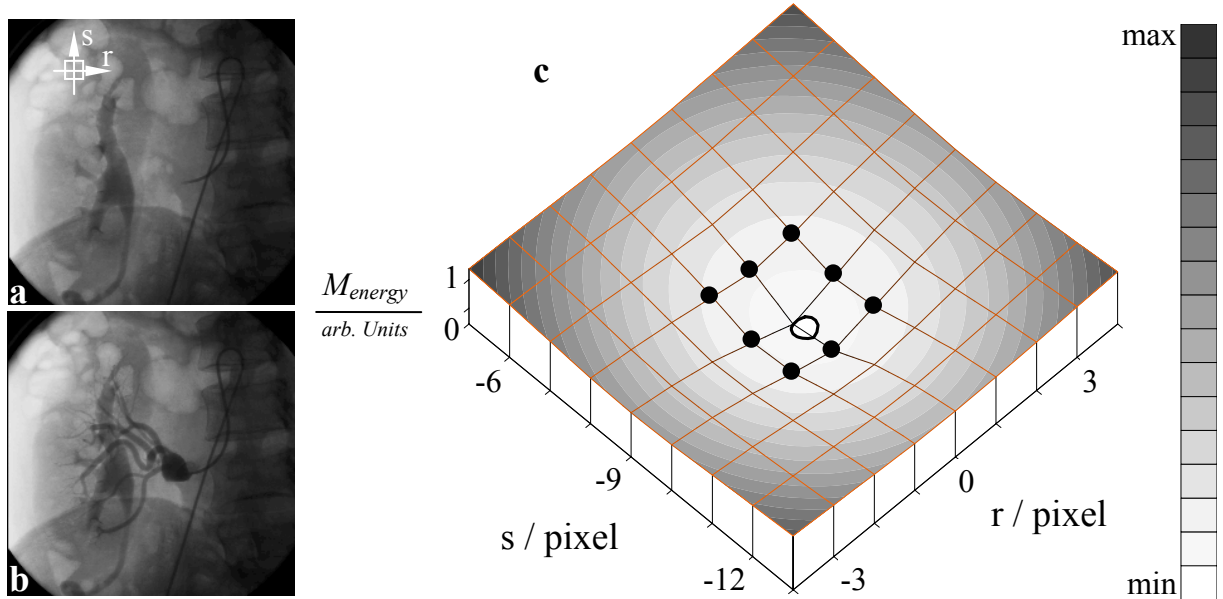


Figure 1: Mask (a) and contrast image (b) of an fluoroscopic image pair of the abdomen. The quadratic template and the local coordinate system are indicated in the mask image. Approximated quadratic function (c) from the energy similarity measure. The grid shows the pixel-accurate values of the inverted energy. In the 8-neighbourhood (indicated with black points) of the point $(r,s)=(0,-9)$ a quadratic function is fitted. This function is gray-value coded and overlaid onto the visible grid of pixel-accurate energy values. It can be seen that the minimum of the quadratic fit is slightly shifted with respect to the energy minimum of the grid.

Fig. 2a/b show the mask and contrast image of the abdomen example introduced above. The vessel tree of a transplanted kidney is investigated. The homologous landmarks are drawn inside the indicated rectangular region-of-interest and the motion vector field is indicated in the contrast image. For better visualization both regions are blown up. The set of homologous sub-pixel landmarks (i.e. the template centers, sometimes also called *control points*) resulting from the template matching is straightforwardly used to estimate the parameters of an appropriate transformation f relating the points of the mask image to the corresponding points in the contrast image inside the region-of-interest:

$$(x', y') \rightarrow (x, y) = (f_x(x', y'), f_y(x', y')), \quad (3)$$

where (x', y') and (x, y) are the coordinates of the contrasted image and the mask image, respectively.

In clinical routine the function f in eq. (3) is the pure shift transformation. As improvement of this situation mask and contrast image may be subtracted inside the region-of-interest after motion correction with an affine transformation that allows for the compensation of shift, scale, rotation as well as skew artifacts and is hence better adapted to the artifacts appearing in clinical practice than the pure shift operation. However, patient motion is often more complex. Therefore, higher-order registration procedures must be applied. In this paper, we present the results of an elastic registration based on Bookstein's thin-plate splines [9,12] which can be considered as an interpolation. The set of homologous landmarks is the same as for the affine transformation, indicated in the mask and in the contrast image of fig. 2. Let $Q_k=(x_k, y_k)$ be a set of points in the mask image and $P_k=(x'_k, y'_k)$ be the corresponding set in the contrast image ($k=1, \dots, N$, where N is the number of landmarks or control points). For the thin-plate spline approach the function f in eq. (3) can be written as

$$f_{\bullet}(x'_{\bullet k}, y'_{\bullet k}) = a_{\bullet 1} + a_{\bullet 2}x'_{\bullet k} + a_{\bullet 3}y'_{\bullet k} + \sum_{j=1}^N w_{\bullet j} U(\|(x'_{\bullet k}, y'_{\bullet k}) - P_j\|), \quad (4)$$

where the point denotes the index for the x- or y-coordinate.

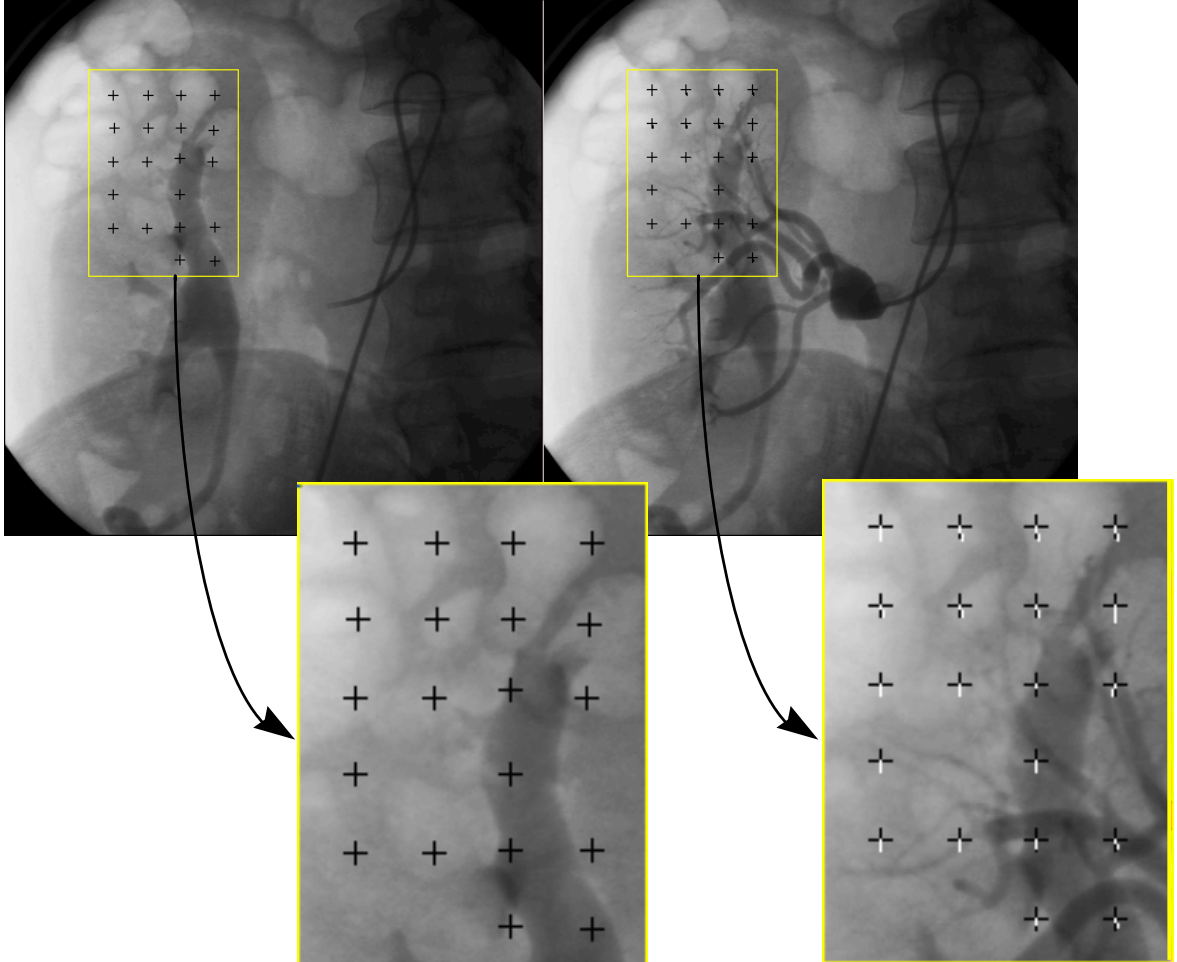


Figure 2: Mask (a) and contrast image (b) of abdomen fluoroscopies showing the success of a kidney transplantation. In the rectangular region-of-interest (blown-up for better visualization in both images) the distribution of landmarks can be seen as black-colored crosses. Additionally, the motion vector field - visualized in the blown-up only - is given by white lines attached to the crosses in the contrast image.

The radial basis function used in the thin-plate approach is

$$U(r) = r^2 \log(r^2), \quad (5)$$

where r is the Euclidean distance $r = (x^2 + y^2)^{1/2}$. In addition to these equations, the method also requires the boundary conditions

$$\sum_{k=1}^N w_{\bullet k} = 0, \quad \sum_{k=1}^N w_{\bullet k} x_k = 0 \quad \text{and} \quad \sum_{k=1}^N w_{\bullet k} y_k = 0. \quad (6)$$

where $w_{\bullet k}$ are the parameters of the elastic components of the registration. The boundary conditions ensure that terms are removed that grow faster than linear terms as one moves far away from the data. The set of equations (4) is solved by singular value decomposition [11].

Fig. 3 shows the results of the interactively applied global shift (a), the affine transformation (b), and the elastic transformation (c) applied to the mask image prior to subtraction. The patient-induced distortions, visible in fig. 3a, can be significantly reduced by application of the affine transformation (fig. 3b). However, especially for the presented abdominal images residual artifacts (e.g. indicated with an arrow in the affinely corrected region) are visible in the subtraction image even after an affine correction.

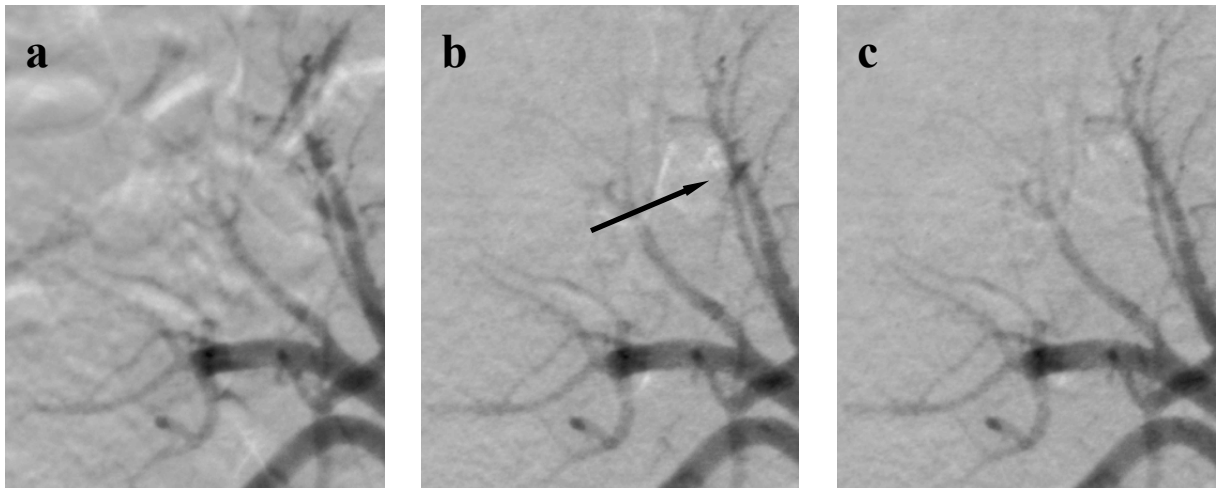


Figure 3: Subtraction results for the manually shifted correction (a) compared with the affinely (b) and elastically corrected (c) region-of-interest indicated in fig.2. The arrow in the affinely corrected DSA image marks an example for a residual artifact that vanishes in the elastically corrected image.

3. CONCLUSIONS

We compared the quality of digital subtraction angiography images that underwent different motion correction procedures prior to subtraction. A global interactive shift corrected mask as well as an affinely and an elastically motion corrected mask are used to enhance the quality of the subtraction images. The latter two approaches are based on motion vector fields that are obtained from a template matching procedure optimizing a histogram-based energy measure. The motion vector field is given in sub-pixel accuracy obtained from an approximation of the objective function with a quadratic function in the neighbourhood of the pixel extremum. For the abdomen fluoroscopy example, selected in the present paper to illustrate the results, it becomes evident that pure shift operations and also affine transformations cannot cope with the flexible motion that typically occurs in abdominal regions. Therefore, a thin-plate spline approach is used to achieve a further enhancement of the subtraction images. Thanks to the smooth, sub-pixel accurate motion vector field that is estimated with the histogram-based energy similarity measure, the application of the thin-plate spline interpolation is possible without specific efforts for outlier treatment.

ACKNOWLEDGMENT

The authors would like to thank Dr. L. J. Schultze Kool, University Hospital Leiden, for providing us with the data sets. The algorithm was implemented on an experimental version of the EasyVision workstation from Philips Medical Systems and we would like to thank ICS

(EasyVision / EasyGuide) Advanced Development, Philips Medical Systems, Best, for helpful discussions.

REFERENCES

- [1] W. A. Chilcote, M. T. Modic, W. A. Pavlicek et. al., *Digital subtraction angiography of the carotid arteries: A comparative study in 100 patients*, Radiology **139** (1981) 287.
- [2] A. Venot and V. Leclerc, *Automated correction of patient motion and gray values prior to subtraction in digitized angiography*, IEEE Trans. on Med. Im. **4** (1984) 179.
- [3] K. J. Zuiderveld, B. M. ter Haar Romeny and Max. A. Viergever, *Fast rubber sheet masking for digital subtraction angiography*, SPIE **1137** Science and Engineering of Medical Imaging (1989) 22.
- [4] T. M. Buzug and J. Weese, *Improving DSA images with an automatic algorithm based on template matching and an entropy measure*, Proc. of the CAR'96, H. U. Lemke, M. W. Vannier, K. Inamura and A. G. Farman (Eds.), (Elsevier, Amsterdam, 1996) p. 145.
- [5] T. M. Buzug, J. Weese, C. Fassnacht and C. Lorenz, *Using an entropy similarity measure to enhance the quality of DSA images with an algorithm based on template matching*, in: Proc. of the 4th Int. Conf. on VBC'96, Lecture Notes in Computer Science **1131** (Springer, Berlin, 1996) p. 235.
- [6] T. M. Buzug, J. Weese, C. Fassnacht and C. Lorenz, *Image registration: Convex-weighted functions for histogram-based similarity measures*, Proc. of the CVRMed/MRCAS'97, Lecture Notes in Computer Science **1205** (Springer, Berlin, 1997) p. 203.
- [7] A. Rosenfeld and A. Kak, *Digital picture processing*, 2nd ed. (Academic Press, New York, 1982).
- [8] J. M. Fitzpatrick, J. J. Grefenstette, D. R. Pickens, M. Mazer and J. M. Perry, *A system for image registration in digital subtraction angiography*, in: Information processing in medical imaging, C. N. de Graaf and M. A. Viergever (eds.), (Plenum Press, New York, 1988) p. 414.
- [9] F. L. Bookstein, *Principal warps: Thin-plate splines and the decomposition of deformations*, IEEE Trans. PAMI **11** (1989) 567.
- [10] M. Yanagisawa, S. Shigemitsu and T. Akatsuka, *Registration of locally distorted images by multiwindow pattern matching and displacement interpolation: The proposal of an algorithm and its application to digital subtraction angiography*, in 7th Int. Conf. of Pattern Recognition (IEEE Computer Society Press, Silver Spring Md., 1984) p. 1288.
- [11] W. H. Press, B. P. Flannery, S. A. Teukolsky and W. T. Vetterling, *Numerical Recipes in C* (Cambridge University Press, Cambridge, 1990) p. 534.
- [12] K. Rohr, H. S. Stiehl, R. Sprengel, W. Beil, T. M. Buzug, J. Weese and M. H. Kuhn: *Point-Based Elastic Registration of Medical Image Data Using Approximating Thin-Plate Splines*. In: Proc. of the 4th Int. Conf. on VBC'96, Lecture Notes in Computer Science **1131** (Springer, Berlin, 1996) p. 297.